Inorganic Chemistry

including bioinorganic chemistry

May 6, 2013
Volume 52, Number 9
pubs.acs.org/IC

Metal–ligand multiple bonds meet metal–metal bonds

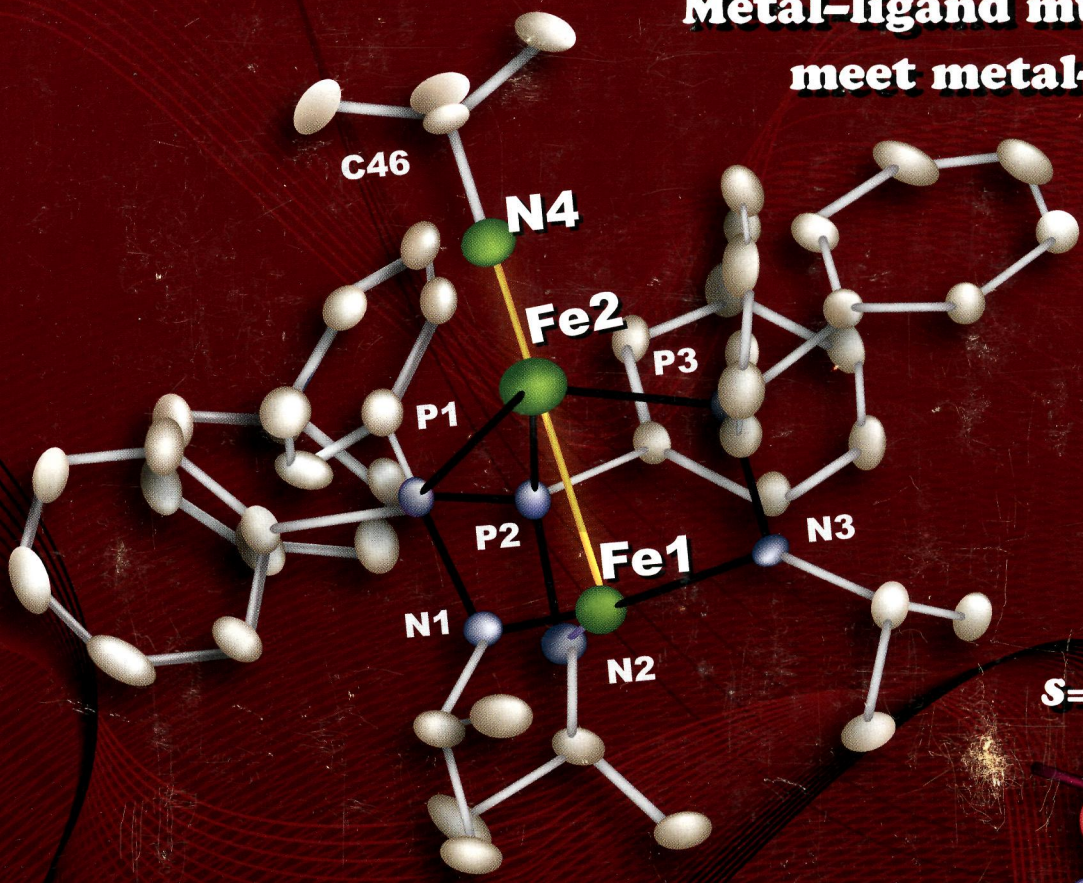

S=5/2 diiron imido

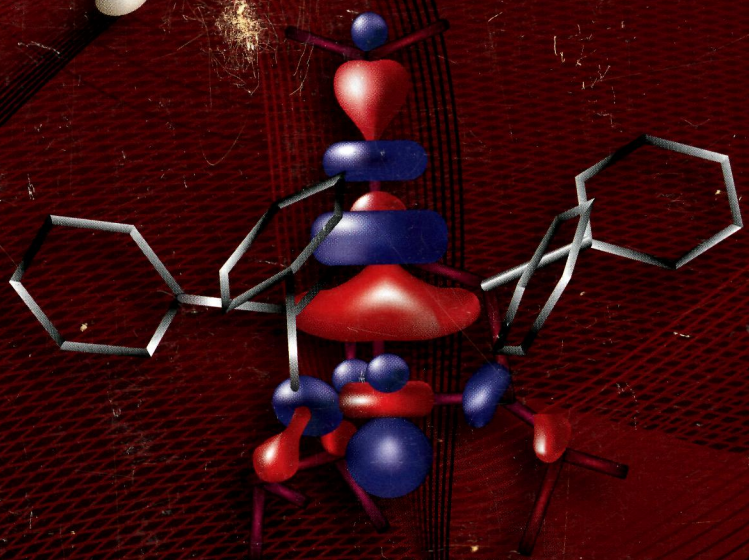

ACS Publications
MOST TRUSTED. MOST CITED. MOST READ.

www.acs.org

Inorganic Chemistry

MAY 6, 2013
VOLUME 52 ISSUE 9

INOCAJ 52(9) 4747–5620 (2013)
ISSN 0020-1669
Registered in the U.S. Patent and Trademark Office

ON THE COVER: The mixed-valence $Fe^{II}Fe^{III}$ imido complex shown is an unusual example of a first-row bimetallic complex featuring both metal–metal bonds and metal–ligand multiple bonds. The high-spin nature of the pendent Fe^{II} center leads to an overall $S = 5/2$ system with highly delocalized bonding. See S. Kuppuswamy, T. M. Powers, B. M. Johnson, M. W. Bezpalko, C. K. Brozek, B. M. Foxman, L. A. Berben, and C. M. Thomas, p 4802.

Communications

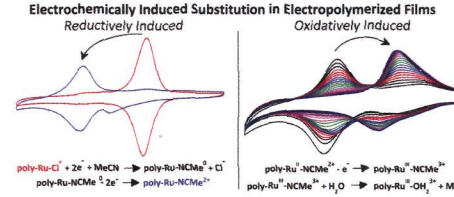

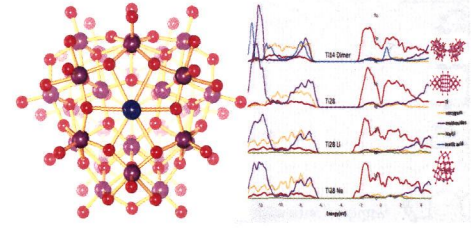

4753 S dx.doi.org/10.1021/ic4001945

Cobalt Polyoxometalates as Heterogeneous Water Oxidation Catalysts

Joaquín Soriano-López, Sara Goberna-Ferrón, Laura Vigara, Jorge J. Carbó, Josep M. Poblet, and José Ramón Galán-Mascarós*

The homogeneous water oxidation catalyst $[Co_9(H_2O)_6(OH)_3(HPO_4)_2(PW_9O_{34})_3]^{16-}$ (Co_9) maintains its redox activity when incorporated into a solid-state matrix. As part of a modified amorphous carbon electrode, high catalytic water oxidation rates are maintained for hours in a large pH range, including acidic conditions, where classic metal oxides are unstable.

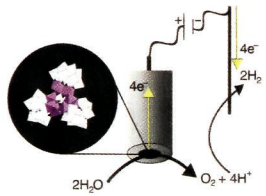

4756 S dx.doi.org/10.1021/ic400211s

Tight Encapsulation of a "Naked" Chloride in an Imidotitanium Hexanuclear Host

Christian Lorber* and Laure Vendier

The base-free hexanuclear complex $[\{Ti(=NAr)Cl_2\}_6(Cl)]^-[Q]^+$ [$Q^+ = Me_2NHSiMe_3^+$ and $Me_2N(SiMe_3)_2^+$] is obtained by treating the imidotitanium dimer $[Ti(\mu\text{-}NAr)(NMe_2)_2]_2$ (Ar = 2,6-^{i}Pr$_2$C$_6$H$_3$) with excess Me_3SiCl. The self-assembled hexameric cage arrangement encapsulates a chloride ion guest.

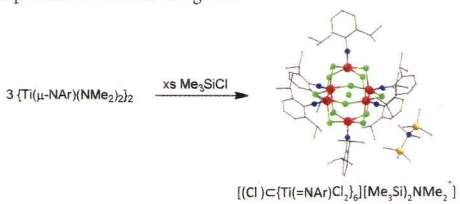

4759 S dx.doi.org/10.1021/ic400285a

Bilayer Mott System with Cation···Anion Supramolecular Interactions Based on a Nickel Dithiolene Anion Radical: Coexistence of Ferro- and Antiferromagnetic Anion Layers and Large Negative Magnetoresistance

Tetsuro Kusamoto,* Hiroshi M. Yamamoto, Naoya Tajima, Yugo Oshima, Satoshi Yamashita, and Reizo Kato

A novel bilayer Mott system, $(Et\text{-}4BrT)[Ni(dmit)_2]_2$ (Et-4BrT = ethyl-4-bromothiazolium; dmit = 1,3-dithiole-2-thione-4,5-dithiolate), contains two nonequivalent $Ni(dmit)_2$ anion layers, where both layers form Mott insulating states. Supramolecular $Br_{cation}\cdots S_{anion}$ and $S_{cation}\cdots S_{anion}$ interactions play a crucial role in constructing the bilayer structure. The ferro- and antiferromagnetic short-range-ordering layers coexist in the crystal, which achieves large negative magnetoresistance ($\Delta\rho/\rho_0 \approx -75\%$ at 70 kOe) at 5 K under 1 GPa.

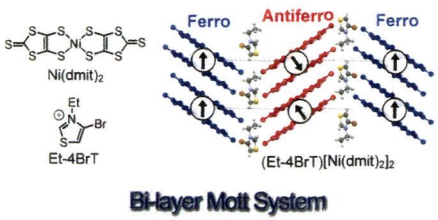

4762 S dx.doi.org/10.1021/ic400290a

Open-Shell Triplet Character of $^{\#6094}C_{68}$: Spherical Aromaticity, Thermodynamic Stability, and Regioselective Chlorination

Jing-Shuang Dang, Jia-Jia Zheng, Wei-Wei Wang, and Xiang Zhao*

The recently captured fullerene $^{\#6094}C_{68}$ with an open-shell triplet ground state was found to exhibit unexpected triplet aromaticity, excellent thermodynamic stability, and a regioselective exohedral chlorination pattern, according to the density functional theory calculations.

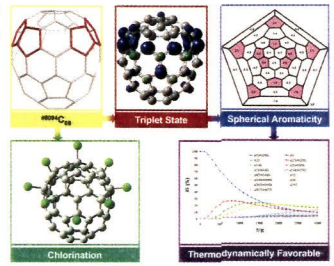

4765 S dx.doi.org/10.1021/ic400315g

Solvent-Soluble Coordination Polymer That Reconstructs Cyclic Frameworks That Trap a Kinetically Labile $[Cu(CO_3)_2]^{2-}$ Unit

Tatsunari Inoue, Katsunori Yamanishi, and Mitsuru Kondo*

A new 2D coordination polymer, which was obtained by the treatment of a bis-imidazole-type ligand with basic copper(II) carbonate or copper(II) hydroxide, was structurally characterized. This compound converted to new pentanuclear complexes with cyclic frameworks, which trapped a kinetically labile $[Cu(CO_3)_2]^{2-}$ unit. Their conversion reactions were studied by absorption and ESI-TOF mass spectrometry.

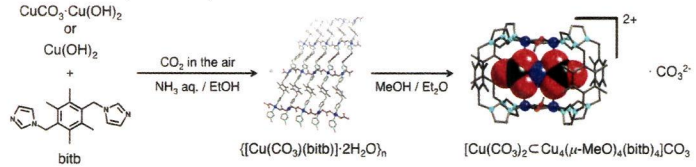

4768 S dx.doi.org/10.1021/ic400358e

Trifluoromethyl and Chloro Derivatives of a Higher Fullerene D_2-C_{80}(2): $C_{80}(CF_3)_{12}$ and $C_{80}Cl_{28}$

Shangfeng Yang,* Tao Wei, Nadezhda B. Tamm, Erhard Kemnitz, and Sergey I. Troyanov*

Two derivatives of the low-abundant D_2-C_{80} (isomer 2), $C_{80}(CF_3)_{12}$ and $C_{80}Cl_{28}$, have been synthesized, isolated, and stucturally elucidated by single-crystal X-ray crystallography. Remarkably, the addition pattern of $C_{80}(CF_3)_{12}$ is the same as that of the known $C_{80}Cl_{12}$. The molecule of $C_{80}Cl_{28}$ (see structure: C, gray; Cl, green) contains very short (1.33 Å) and very long (up to 1.62 Å) C–C bonds in its carbon cage.

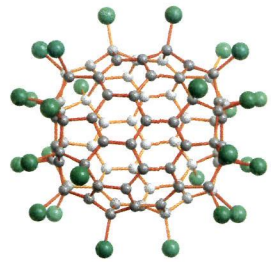

Articles

4786 dx.doi.org/10.1021/ic301539q

Mechanisms of the Water-Gas Shift Reaction Catalyzed by Ruthenium Pentacarbonyl: A Density Functional Theory Study
Hannes Schulz, Andreas Görling, and Wolfgang Hieringer*

The homogeneous water-gas shift reaction catalyzed by $Ru(CO)_5$ is analyzed using density functional methods in solution. Four different mechanistic pathways are considered. Solvent effects turn out to be important for a reasonable comparison among the mechanistic alternatives. The explicit inclusion of a water solvent molecule changes the barriers of certain steps. The results suggest that, depending on the reaction conditions, several pathways may be competitive. Differences and similarities of $Ru(CO)_5$ and $Fe(CO)_5$ catalysis are briefly discussed.

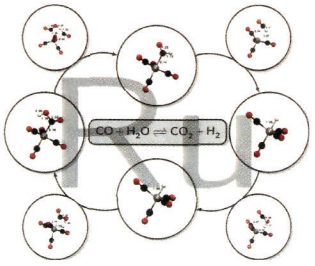

4795 dx.doi.org/10.1021/ic3020892

Regulatory Role of Glu546 in Flavin Mononucleotide — Heme Electron Transfer in Human Inducible Nitric Oxide Synthase
Wenbing Li, Li Chen, Changyuan Lu, Bradley O. Elmore, Andrei V. Astashkin, Denis L. Rousseau, Syun-Ru Yeh, and Changjian Feng*

This work focuses on comparing the electron transfer kinetics and the pulsed EPR properties of the wild type and E546N mutant human iNOS oxygenase/FMN constructs. The results provide an important mechanism by which the FMN *subdomain can modify the interdomain electron transfer between the FMN and the heme centers by altering the probability of* the docked state.

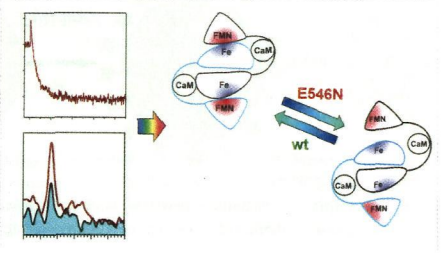

4802 dx.doi.org/10.1021/ic302108k

Metal−Metal Interactions in C_3-Symmetric Diiron Imido Complexes Linked by Phosphinoamide Ligands
Subramaniam Kuppuswamy, Tamara M. Powers, Bruce M. Johnson, Mark W. Bezpalko, Carl K. Brozek, Bruce M. Foxman, Louise A. Berben, and Christine M. Thomas*

The tris(phosphinoamide)-bridged $Fe^{II}Fe^{II}$ diiron complex $Fe(\mu\text{-}^{i}PrNPPh_2)_3Fe(\eta^2\text{-}^{i}PrNPPh_2)$ (**1**) can be reduced in the absence or presence of PMe_3 to generate the mixed-valence $Fe^{II}Fe^{I}$ complex $Fe(\mu\text{-}^{i}PrNPPh_2)_3Fe(PPh_2NH^{i}Pr)$ (**2**) or $Fe(\mu\text{-}^{i}PrNPPh_2)_3Fe(PMe_3)$ (**3**), respectively. Following a typical oxidative group transfer procedure, treatment of **2** or **3** with organic azides generates the mixed-valent $Fe^{II}Fe^{III}$ imido complexes $Fe(^{i}PrNPPh_2)_3Fe{\equiv}NR$ (R = ^{t}Bu (**4**), Ad (**5**), 2,4,6-trimethylphenyl (**6**)).

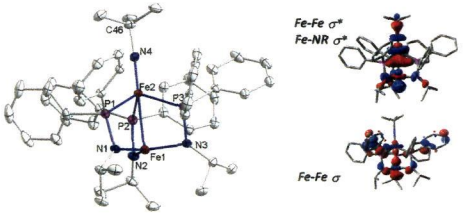

4812 dx.doi.org/10.1021/ic302244e

Site Preference and Ordering Induced by Au Substitution in the γ-Brass Related Complex Au−Cr−Zn Phases
Partha P. Jana,* Ryan Henderson, Bernd Harbrecht, and Sven Lidin

The insertion of gold in the γ-brass related complex binary compound $CrZn_{\sim 17}$ is very site specific and induced gradual ordering in the ternary Au−Cr−Zn phases. At the limiting composition $Au_{10}Cr_4Zn_{89}$ the structure is fully ordered. The crystallographic site occupancy pattern calculated by LDA-DFT parametrized extended Hückel (eH) Mulliken charge populations in the ordered $Au_{10}Cr_4Zn_{89}$ agrees very well with the experimentally found site occupancy pattern.

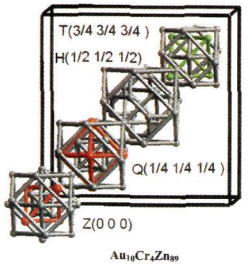

4819 dx.doi.org/10.1021/ic3022485

Molecular Indium(III) Phosphonates Possessing Ring and Cage Structures. Synthesis and Structural Characterization of $[In_2(t\text{-}BuPO_3H)_4(phen)_2Cl_2]$ and $[In_3(C_5H_9PO_3)_2(C_5H_9PO_3H)_4(phen)_3]\cdot NO_3\cdot 3.5H_2O$
Vadapalli Chandrasekhar,* Joydeb Goura, and Andrew Duthie

Two novel indium(III) phosphonates, $[In_2(t\text{-}BuPO_3H)_4(phen)_2Cl_2]$ (**1**) and $[In_3(C_5H_9PO_3)_2(C_5H_9PO_3H)_4(phen)_3]\cdot NO_3\cdot 3.5H_2O$ (**2**) with phen = 1,10-phenanthroline, have been synthesized by *solvothermal reactions involving indium(III) salts and organophosphonic acids. 1 is a dinuclear compound where the two* indium centers are bridged by a pair of isobidentate phosphonate ligands, $[t\text{-}BuP(O)_2OH]^-$, resulting in an eight-membered $(In_2P_2O_4)$ puckered ring. Compound **2** is trinuclear; the In_3 platform is held together by two bicapping tripodal phosphonate ligands from the top and bottom of the indium plane.

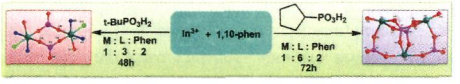

4825 dx.doi.org/10.1021/ic302259t

Phenolate- and Acetate (Both μ_2-1,1 and μ_2-1,3 Modes)-Bridged Linear Co^{II}_3 and $Co^{II}_2Mn^{II}$ Trimers: Magnetostructural Studies
Anuj Kumar Sharma, Francesc Lloret, and Rabindranath Mukherjee*

Comparative magnetostructural studies have been made among five linear trimers supported by uncommon phenoxide and two types of acetate bridges. Barring $Ni^{II}_2Mn^{II}$, which is antiferromagnetic ($J = -0.30$ cm^{-1}), all are ferromagnetic (J values: +1.20 to +0.71 cm^{-1}). The subtle fine-tuning that triggers changes in the nature and extent of magnetic-exchange interaction has been rationalized. The trimer formation has been justified by the structural characterization of a Ni^{II} monomer precursor.

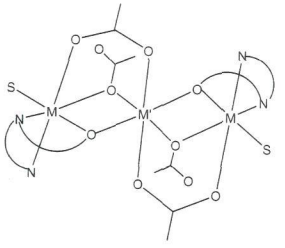

4880 S dx.doi.org/10.1021/ic302459z

Emission, Raman Spectroscopy, and Structural Characterization of Actinide Tetracyanometallates

Branson A. Maynard, K. Sabrina Lynn, Richard E. Sykora, and Anne E. V. Gorden*

Three new compounds $\{U_2(H_2O)_{10}(O)[Pt(CN)_4]_3\}\cdot 4H_2O$, $\{Th_2(H_2O)_{10}(OH)_2[Pd(CN)_4]_3\}\cdot 8H_2O$, and $\{(UO_2)_2(DMSO)_4(OH)_2[Ni(CN)_4]\}$ were characterized by confocal Raman spectroscopy and single crystal XRD. The absence of significant emission in the visible range compared to the platinum starting material for $\{U_2(H_2O)_{10}(O)[Pt(CN)_4]_3\}\cdot 4H_2O$ is unusual because of the presence of the one-dimensional Pt···Pt chains in this compound. Confocal Raman spectroscopy of the cyanide stretching region provides insight into the binding domain (mono-, bi-, tri-, tetradentate) of the tetracyanometallates in these structures.

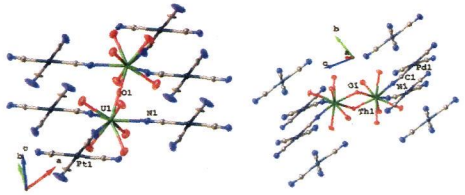

4890 S dx.doi.org/10.1021/ic302478e

Switching of Reverse Charge Transfers for a Rational Design of an OFF–ON Phosphorescent Chemodosimeter of Cyanide Anions

Jean-Luc Fillaut,* Huriye Akdas-Kilig, Edouard Dean, Camille Latouche, and Abdou Boucekkine*

We describe a new luminescence-enhanced anion sensor mechanism based on an inversion of metal-to-ligand and ligand-to-ligand charge transfers in a neutral cyclometalated phenylbipyridyl Pt(II) acetylide, so that its luminescence is dramatically activated concomitantly with selective and sensitive responses to various concentrations of cyanide anion.

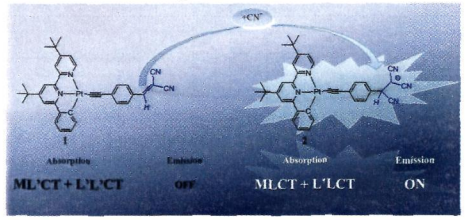

4898 S dx.doi.org/10.1021/ic3024887

Long-Range Intramolecular Electronic Communication in Bis(ferrocenylethynyl) Complexes Incorporating Conjugated Heterocyclic Spacers: Synthesis, Crystallography, and Electrochemistry

Hakikulla H. Shah, Rayya A. Al-Balushi, Mohammed K. Al-Suti, Muhammad S. Khan,* Christopher H. Woodall, Kieran C. Molloy, Paul R. Raithby,* Thomas P. Robinson, Sara E. C. Dale, and Frank Marken*

A series of bis(ferrocenylethynyl) complexes in which the iron centers communicate via a range of conjugated heterocylic spacers have been synthesized, and the interaction between metals has been probed by spectroelectrochemical methods.

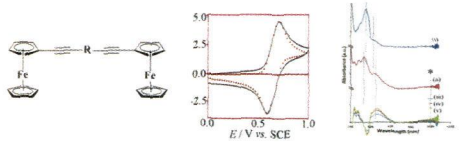

4909 S dx.doi.org/10.1021/ic3024925

Structure and Unusual Magnetic Properties of $YbMn_{0.17}Si_{1.88}$

Sebastian C. Peter, Christos D. Malliakas, and Mercouri G. Kanatzidis*

Single crystals of $YbMn_{0.17}Si_{1.88}$ grow in an indium flux. $YbMn_{0.17}Si_{1.88}$ crystallizes in the rare monoclinic polar space group $P2_1$. Magnetic susceptibility measurements suggest that the ytterbium atoms in $YbMn_xSi_{2-x}$ may exist in a mixed valent or intermediate valent state, and heat capacity data suggest moderate heavy fermion behavior.

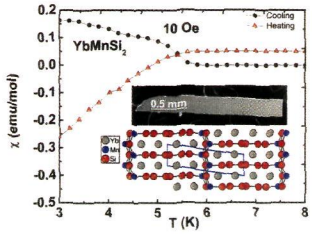

4916 S dx.doi.org/10.1021/ic302510p

Syntheses, Photoluminescence, and Electroluminescence of a Series of Iridium Complexes with Trifluoromethyl-Substituted 2-Phenylpyridine as the Main Ligands and Tetraphenylimidodiphosphinate as the Ancillary Ligand

Qiu-Lei Xu, Cheng-Cheng Wang, Tian-Yi Li, Ming-Yu Teng, Song Zhang, Yi-Ming Jing, Xu Yang, Wei-Nan Li, Chen Lin, You-Xuan Zheng,* Jing-Lin Zuo, and Xiao-Zeng You

The number and positions of the trifluoromethyl groups at the phenyl ring of 2-phenylpyridine greatly affected the emission spectra of Ir^{3+} complexes. With these complexes as the emitters, respectively, the OLEDs [TAPC (30 nm)/Ir (x wt %):SimCP2 (15 nm)/TPBi (45 nm)/LiF (1 nm)/Al (100 nm)] showed good performances with a maximum luminance of over 39000 cd m^{-2} and maximum luminance efficiency (η_L) and power efficiency (η_p) of 50.8 cd A^{-1} and 29.0 lm W^{-1}, respectively.

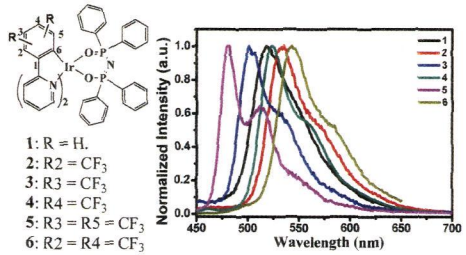

4926 S dx.doi.org/10.1021/ic302531t

Heterobimetallic Lantern Complexes That Couple Antiferromagnetically through Noncovalent Pt···Pt Interactions

Frederick G. Baddour, Stephanie R. Fiedler, Matthew P. Shores, James A. Golen, Arnold L. Rheingold, and Linda H. Doerrer*

A series of Pt-based heterobimetallic lantern complexes of the form $[PtM(SAc)_4L]$ (L = OH_2, 3-NO_2py; M = Co, Ni, Zn) has been prepared. All compounds exist as dimeric species formed by two unbridged lantern units linked by a noncovalent Pt···Pt interaction that serves as a pathway for antiferromagnetic coupling between paramagnetic 3d metal centers.

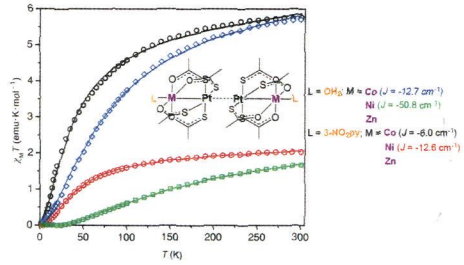

4934 dx.doi.org/10.1021/ic302525k

Hydrothermal Synthesis and Structural and Spectroscopic Properties of the New Triclinic Form of $GdBO_3$:Eu^{3+} Nanocrystals

Agata Szczeszak, Tomasz Grzyb, Bolesław Barszcz, Vitali Nagirnyi, Aleksei Kotlov, and Stefan Lis*

Triclinic $Gd_{1-x}Eu_xBO_3$ nanophosphors have been prepared by a hydrothermal method without using additional coreagents and prior precipitation of precursor (*in situ*). The formation of the borate nanorods and their crystal structure was refined on the basis of X-ray diffraction patterns (XRD) and well confirmed using various techniques such as infrared spectroscopy (IR), Raman spectroscopy, transmission electron microscopy (TEM), and energy-dispersive X-ray spectroscopy (EDX).

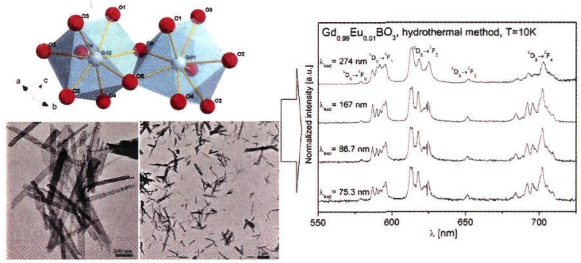

4941 dx.doi.org/10.1021/ic302587t

Crystal Growth and First Crystallographic Characterization of Mixed Uranium(IV)−Plutonium(III) Oxalates

Christelle Tamain, Bénédicte Arab Chapelet, Murielle Rivenet,* Francis Abraham, Richard Caraballo, and Stéphane Grandjean

The first mixed-actinide uranium(IV)−plutonium(III) oxalate single crystals, $(NH_4^+)_{0.5}[Pu^{III}_{0.5}U^{IV}_{0.5}(C_2O_4)_2{\cdot}H_2O]{\cdot}3.5H_2O$ (**1**) and $(NH_4^+)_{2.7}Pu^{III}_{0.7}U^{IV}_{1.3}(C_2O_4)_5{\cdot}nH_2O$ (**2**), have been prepared by the slow diffusion of reagents through membranes in a specially designed diffusion cell. UV−vis, Raman, and thermal ionization mass spectrometry analyses on both single crystals demonstrate the presence of both metallic cations with conservation of the oxidation state and the formation of mixed oxalate structures that belong to the tetragonal and hexagonal series of mixed oxalates.

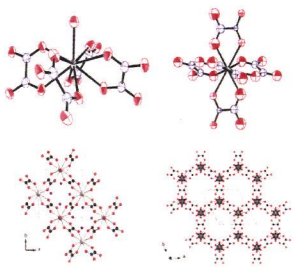

4950 dx.doi.org/10.1021/ic302594b

Improving the Photosensitizing Properties of Ruthenium Polypyridyl Complexes Using 4-Methyl-2,2′-bipyridine-4′-carbonitrile as an Auxiliary Ligand

Juan H. Mecchia Ortiz, Nadia Vega, David Comedi, Mónica Tirado, Isabel Romero, Xavier Fontrodona, Teodor Parella, F. Eduardo Morán Vieyra, Claudio D. Borsarelli, and Néstor E. Katz*

A new series of complexes of formula $[Ru(bpy)_{3-x}(Mebpy\text{-}CN)_x](PF_6)_2$ (x = 1−3) (bpy =2,2′-bipyridine, Mebpy-CN = 4-methyl-2,2′-bipyridine-4′-carbonitrile) has been prepared and characterized by physicochemical techniques. Quenching of their excited states by molecular oxygen produced $^1O_2$ with higher quantum yields than that of $[Ru(bpy)_3]^{2+}$. Photoconductivity of ZnO nanowires is enhanced by soaking them in a concentrated solution of the complex with x = 1. A new mixed-valent dinuclear species of formula $[(bpy)_2Ru^{II}(Mebpy\text{-}CN)Ru^{III}(NH_3)_5]^{5+}$ is also described.

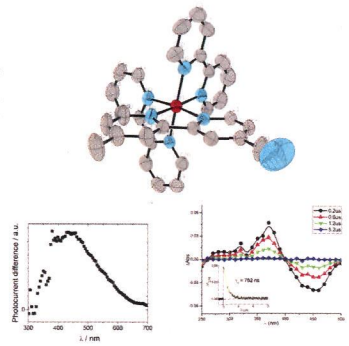

4963 dx.doi.org/10.1021/ic302598d

Aromatic Chelator-Specific Lattice Architecture and Dimensionality in Binary and Ternary Cu(II)-Organophosphonate Materials

V. Georgantas, M. Menelaou, V. Psycharis, C. P. Raptopoulou, A. Terzis, V. Tangoulis, C. Mateescu, and A. Salifoglou*

pH-Specific stoichiometric reactions of Cu(II), butylene diamine tetra(methylenephosphonic acid) (H_8BDTMP), and py/phen led to the isolation of the first Cu(II)-BDTMP species $Na_6[Cu_2(BDTMP)(H_2O)_4]{\cdot}[Cu_2(BDTMP)(H_2O)_4]_{0.5}{\cdot}26H_2O$ (**1**), $[Cu_2(H_4BDTMP)(py)_4]{\cdot}2H_2O$ (**2**), and $[Cu_2(phen)_2(H_4BDTMP)]_n{\cdot}6.6nH_2O{\cdot}1.5n$MeOH (**3**). Analytical, spectroscopic, magnetic, and structural studies formulate the physicochemical profile of these new binary/ternary species, (a) shedding light onto aqueous/nonaqueous Cu(II)−organophosphonate interactions and (b) projecting the influence of structural and physicochemical factors on the binary/ternary Cu(II)−organophosphonate lattice architecture of novel materials with defined 2D−3D dimensionality.

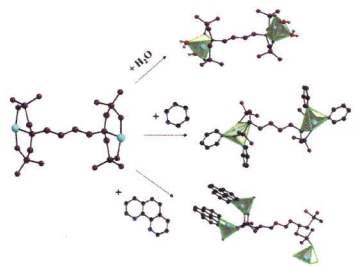

4977 dx.doi.org/10.1021/ic3026232

$Sr_7Co_4(CO_3)O_{13-\delta}$ (δ = 1.64), An Original Cobaltite Derivative of the Ruddlesden–Popper Series

A. Demont, D. Pelloquin,* S. Hébert, M. Hervieu, J. Höwing, and A. Maignan

This material has been characterized by combining transmission electron microscopy analyses and neutron diffraction. Its crystal structure consists of a regular intergrowth between the carbonated m = 3 and m = 2 members of the $Sr_{n+1}Co_nO_{3n+1}$ Ruddlesden–Popper (RP) series, $Sr_4Co_2(CO_3)O_{5.49}$ and $Sr_3Co2O_{5.87}$, respectively. Magnetotransport measurements evidence a semiconducting behavior and complex magnetic interactions with four specific transitions that can be ascribed to mixed valence II/III of cobalt species resulting from the large oxygen nonstoichiometry.

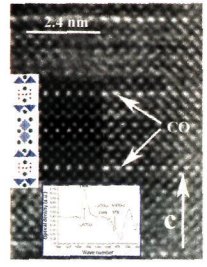

4985 dx.doi.org/10.1021/ic302678b

Ruthenium Complexes with Chiral Bis-Pinene Ligands: an Array of Subtle Structural Diversity

Lydia Vaquer, Albert Poater, Jonathan De Tovar, Jordi García-Antón, Miquel Solà, Antoni Llobet,* and Xavier Sala*

A new chiral Ru-based derivative of the *N*,*N*-bis(2-pyridylmethyl)ethylamine (bpea) ligand has been prepared from a new pineno-fused aldehyde building block arising from the monoterpene chiral pool. The tridentate ligand has been employed to prepare a new set of isomeric Ru–Cl complexes in combination with the didentate 2,2′-bipyridine (bpy) ligand. Both the structural diversity of this family of complexes and the isomerization processes taking place among them have been studied and rationalized, in terms of electronic and steric effects, by means of DFT calculations.

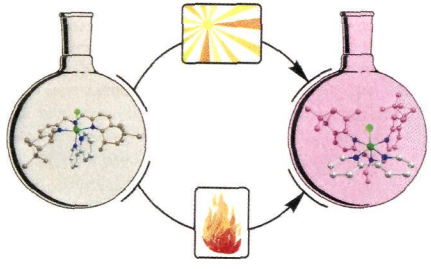

4993 dx.doi.org/10.1021/ic3026842

BTBPs versus BTPhens: Some Reasons for Their Differences in Properties Concerning the Partitioning of Minor Actinides and the Advantages of BTPhens

Frank W. Lewis,* Laurence M. Harwood,* Michael J. Hudson, Michael G. B. Drew, Véronique Hubscher-Bruder, Vladimira Videva, Françoise Arnaud-Neu, Karel Stamberg, and Shyam Vyas

Two members of the tetradentate *N*-donor 6,6′-bis(1,2,4-triazin-3-yl)-2,2′-bipyridine (BTBP) and 2,9-bis(1,2,4-triazin-3-yl)-1,10-phenanthroline (BTPhen) ligand families currently being developed for separating actinides from lanthanides have been studied by a combination of density functional theory calculations, lanthanide NMR spectroscopic titrations and lanthanide-binding competition experiments, spectrophotometric and microcalorimetric titrations with lanthanides in solution, and X-ray crystallography.

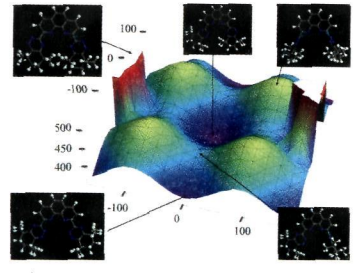

5006 dx.doi.org/10.1021/ic302694y

Metal Atom Lability in Polynuclear Complexes

Emily V. Eames, Raúl Hernández Sánchez, and Theodore A. Betley*

Facile metal atom metathesis was observed for the open-shell clusters while maintaining cluster morphology. The oxidized cluster $[(^{Ph}L)Fe_3(\mu\text{-}Cl)]_2$ reacts with $CoCl_2$ to afford trinuclear products where one or two irons, respectively, can be substituted. Metal atom substitution was verified by ^1H NMR, ^{57}Fe Mossbauer, single crystal X-ray diffraction, X-ray fluorescence, and magnetometry analysis. Spectroscopic analysis revealed that the Co atom(s) substitute(s) into the oxidized dimetal unit ($[M_2]^{5+}$), while the M^{2+} site remains iron-substituted.

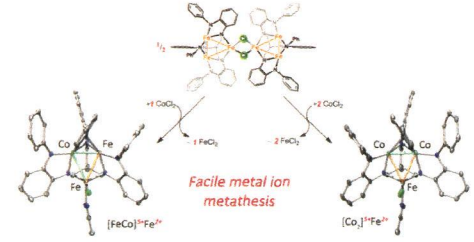

5013 dx.doi.org/10.1021/ic302726z

Crystal Structure and Highly Luminescent Properties Studies of Bis-β-diketonate Lanthanide Complexes

Jing Shi, Yanjun Hou,* Wenyi Chu, Xiaohong Shi, Huiquan Gu, Bilin Wang, and Zhizhong Sun*

A new bis-β-diketonate, 1,3-bis(4,4,4-trifluoro-1,3-dioxobutyl)phenyl (BTP), has been designed and employed for the synthesis of two series of new BTP lanthanide complexes which feature promising luminescence quantum yield and lifetime.

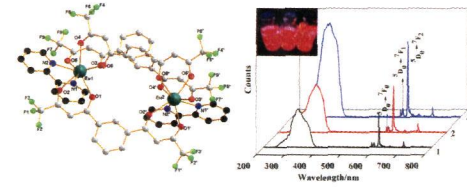

5023 dx.doi.org/10.1021/ic3027336

Tetrathiafulvalene-1,3,5-triazines as (Multi)Donor–Acceptor Systems with Tunable Charge Transfer: Structural, Photophysical, and Theoretical Investigations

Flavia Pop, François Riobé, Sabine Seifert, Thomas Cauchy, Jie Ding, Nathalie Dupont, Andreas Hauser,* Marius Koch, and Narcis Avarvari*

Covalently linked tetrathiafulvalene-1,3,5-triazine (TTF-TZ) systems, with planar solid-state structures for the monoTTF derivatives, possess intramolecular charge transfer (ICT) modulated by the substitution scheme on TZ, as experimentally and theoretically evidenced, while photophysical studies show redox tunable luminescent properties for a C_3 symmetric derivative.

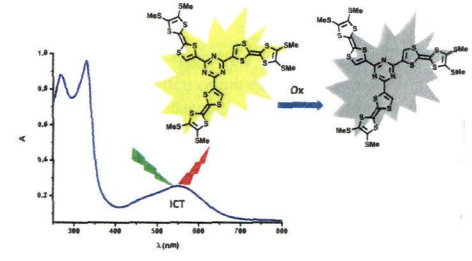

5035 S dx.doi.org/10.1021/ic302742u

Synthesis, Structure, and Magnetic Properties of a New Family of Tetra-nuclear $\{Mn_2^{III}Ln_2\}$(Ln = Dy, Gd, Tb, Ho) Clusters With an Arch-Type Topology: Single-Molecule Magnetism Behavior in the Dysprosium and Terbium Analogues

Vadapalli Chandrasekhar,* Prasenjit Bag, Manfred Speldrich, Jan van Leusen, and Paul Kögerler*

Sequential reaction of Mn(II) and lanthanide(III) salts with a new multidentate ligand, 2,2′-(2-hydroxy-3-methoxy-5-methylbenzylazanediyl)diethanol ($\mathbf{LH_3}$), containing two flexible ethanolic arms, one phenolic oxygen, and a methoxy group afforded heterometallic tetranuclear complexes $[Mn_2Dy_2(LH)_4(\mu\text{-}OAc)_2](NO_3)_2\cdot 2CH_3OH\cdot 3H_2O$ (**1**), $[Mn_2Gd_2(LH)_4(\mu\text{-}OAc)_2](NO_3)_2\cdot 2CH_3OH\cdot 3H_2O$ (**2**), $[Mn_2Tb_2(LH)_4(\mu\text{-}OAc)_2](NO_3)_2\cdot 2H_2O\cdot 2CH_3OH\cdot Et_2O$ (**3**) and $[Mn_2Ho_2(LH)_4(\mu\text{-}OAc)_2]Cl_2\cdot 5CH_3OH$ (**4**). All of these dicationic complexes possess an arch-like structural topology containing a central Mn^{III}–Ln–Ln–Mn^{III} core. The two central lanthanide ions are connected via two phenolate oxygen atoms.

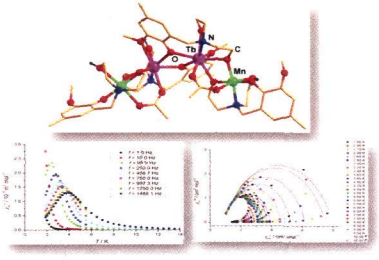

5045 S dx.doi.org/10.1021/ic302769h

Structure, Phase Transition Behaviors and Electrical Properties of Nd Substituted Aurivillius Polycrystallines $Na_{0.5}Nd_xBi_{2.5-x}Nb_2O_9$ (x = 0.1, 0.2, 0.3, and 0.5)

Changbai Long, Huiqing Fan, and Pengrong Ren*

The isovalent substitution of Nd for Bi induced excellent piezoelectric properties of the NDBN0.2 and NDBN0.3, which originated from the reduction of defects (mainly oxygen vacancies in the perovskite layers), the depression of the leakage current, and a sound grain growth. However, an excess Nd substitution results in a dramatic decrease in d_{33} of NDBN0.5, because of a decrease in orthorhombicity polarization and outstanding grain-boundary effects accompanying smaller grain size, a higher volume of grain boundaries, and larger internal stresses.

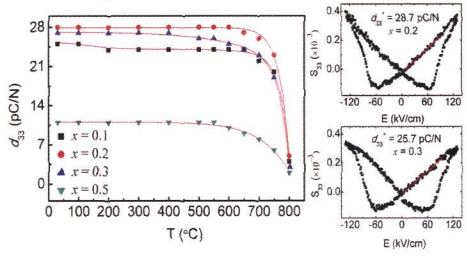

5055 S dx.doi.org/10.1021/ic302805n

Investigation of Fe incorporation in $LnCr_2Al_{20}$ (Ln = La, Gd, Yb) with ^{57}Fe Mössbauer and Single Crystal X-ray Diffraction

LaRico J. Treadwell, Jacob D. McAlpin, Devin C. Schmitt, Michael J. Kangas, Moulay T. Sougrati, Neel Haldolaarachchige, David P. Young, Jean-Claude Jumas, and Julia Y. Chan*

$LnCr_2Al_{20-x}Fe_x$ (Ln = La, Gd, Yb) have been synthesized via flux growth method and characterized with Mössbauer spectroscopy and single crystal X-ray diffraction. $LnCr_2Al_{20}$ (Ln = La, Gd, Yb) are the first with Fe-substituted compounds adopting the $CeCr_2Al_{20}$ structure type. The crystal refinement details and magnetic data of $LnCr_2Al_{20-x}Fe_x$ (Ln = La, Gd, Yb) are reported.

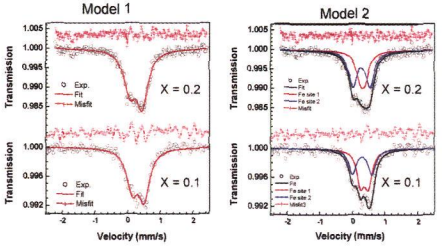

5063 S dx.doi.org/10.1021/ic302831u

Isolation of Elusive Tetranuclear and Pentanuclear M(II)–Hydroximate Intermediates in the Assembly of Lanthanide [15-Metallacrown-5] Complexes

Joseph Jankolovits, Jeff W. Kampf, and Vincent L. Pecoraro*

The first crystal structures of $M^{II}[12\text{-}MC_{M^{II}L}\text{-}4]$ complexes and a tetranuclear 6-MC-2 with Zn(II) metal ions and ligands from the picoline/α-amino hydroximate family are presented. The implications of these compounds as intermediates in metallacrown assembly are discussed.

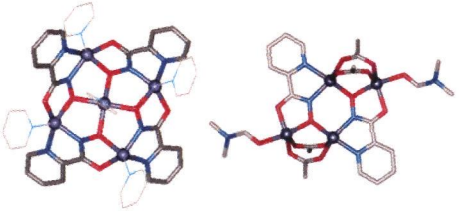

5077 dx.doi.org/10.1021/ic302863h

New Aqua N-Heterocyclic Carbene Ru(II) Complexes with Two-Electron Process as Selective Epoxidation Catalysts: An Evaluation of Geometrical and Electronic Effects

Mohamed Dakkach, Ahmed Atlamsani, Teodor Parella, Xavier Fontrodona, Isabel Romero,* and Montserrat Rodríguez*

A combination of particular electronic and geometrical effects is determining in the occurrence of bielectronic Ru(IV)/Ru(II) redox processes in new ruthenium aquacomplexes containing NHC and polypyridyl ligands. The compounds have been tested in olefin epoxidation, and their performances are discussed on the basis of the electronic properties of the ligands and also of structural factors such as facial/meridional coordination.

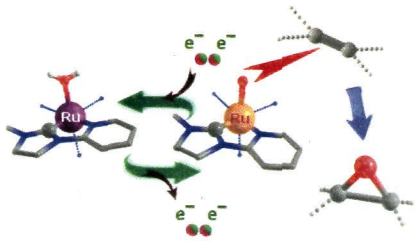

5088 dx.doi.org/10.1021/ic3028644

What Factors Control O_2 Binding and Release Thermodynamics in Mononuclear Ruthenium Water Oxidation Catalysts? A Theoretical Exploration

Guiling Zhang, Kejuan Chen, Hui Chen,* Jiannian Yao, and Sason Shaik

For mononuclear Ru-based water oxidation catalysts (WOCs), our systematic DFT calculations have identified and rationalized that there are several factors that can affect the O_2 release thermodynamics: (1) steric effect from the ligand sphere of Ru; (2) trans effect of ligands trans to O_2; (3) oxygen cis coordinating effect; (4) carbon coordinating effect; and (5) Ru coordination strength. These factors controlling O_2 release thermodynamics shall also affect O_2 release reaction rate via the Bell–Evans–Polanyi (BEP) principle.

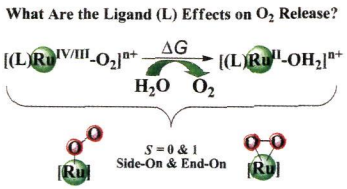

5097 dx.doi.org/10.1021/ic400010d

Carbene Generation by Cytochromes and Electronic Structure of Heme-Iron-Porphyrin-Carbene Complex: A Quantum Chemical Study

Nikhil Taxak, Bhargav Patel, and Prasad V. Bharatam*

The mechanistic pathways for the generation of reactive carbene intermediate from cytochromes and the electronic structure of carbene-heme-iron coordination complex are discussed. The properties of methylenedioxyphenyl (MDP) carbenes are compared with NHCs. MDP-carbenes are sufficiently nucleophilic and form stable (−40.35 kcal/mol) metabolic-intermediate complex (MIC). MIC is stabilized by interaction between carbene-σ_{LP} and empty d_{z^2} orbital of heme-iron. A significant π back-bonding between iron filled d_{xz} orbital and empty p orbital of carbene is also observed.

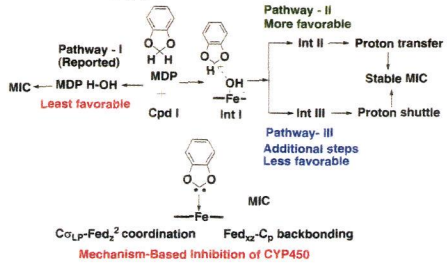

5110 dx.doi.org/10.1021/ic400016z

High Structural Complexity of Potassium Uranyl Borates Derived from High-Temperature/High-Pressure Reactions

Shijun Wu, Shuao Wang, Matthew Polinski, Oliver Beermann, Philip Kegler, Thomas Malcherek, Astrid Holzheid, Wulf Depmeier, Dirk Bosbach, Thomas E. Albrecht-Schmitt,* and Evgeny V. Alekseev*

Three new potassium uranyl borates, $K_{12}[(UO_2)_{19}(UO_4)(B_2O_5)_2(BO_3)_6(BO_2OH)O_{10}]\cdot nH_2O$, $K_4[(UO_2)_5(BO_3)_2O_4]\cdot H_2O$, and $K_{15}[(UO_2)_{18}(BO_3)_3O_{15}]$, were synthesized under high-temperature/high-pressure conditions. Boron exhibits BO_3 coordination only, which is different from other uranyl borates prepared at room temperature or under mild hydrothermal conditions. A rare uranium(VI) tetraoxide core UO_4O_2, which is coordinated by two BO_3 groups, is observed in the structure of the first compound.

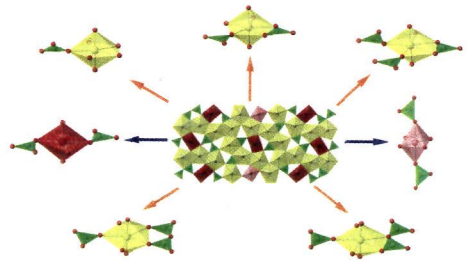

5119 dx.doi.org/10.1021/ic400019r

Novel Antitumor Agent, Trilacunary Keggin-Type Tungstobismuthate, Inhibits Proliferation and Induces Apoptosis in Human Gastric Cancer SGC-7901 Cells

Lu Wang, Bai-Bin Zhou,* Kai Yu, Zhan-Hua Su, Song Gao, Li-Li Chu, Jia-Ren Liu,* and Guo-Yu Yang*

A novel antitumor agent, a one-dimensional chainlike trilacunary Keggin-type tungstobismuthates modified with imi, $[(W(OH)_2)_2(Mn(H_2O)_3)_2(Na_3(H_2O)_{14})(BiW_9O_{33})_2]\cdot(Him)_2\cdot 16H_2O$ (**1**), has been synthesized and structurally characterized, and its biological behavior of inhibiting proliferation and inducing apoptotisis in human gastric cancer SGC-7901 cells in vitro has also been evaluated.

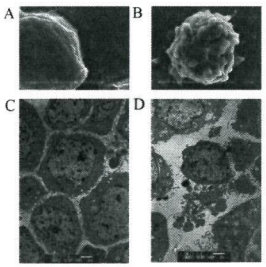

5128 dx.doi.org/10.1021/ic400009m

Tuning the Electronics of Bis(tridentate)ruthenium(II) Complexes with Long-Lived Excited States: Modifications to the Ligand Skeleton beyond Classical Electron Donor or Electron Withdrawing Group Decorations

Giovanny A. Parada, Lisa A. Fredin, Marie-Pierre Santoni, Michael Jäger, Reiner Lomoth, Leif Hammarström, Olof Johansson, Petter Persson, and Sascha Ott*

Substituting the lateral heterocycles from quinoline (green) to *N*-7-azaindole (blue) and quinoxaline (red) has a profound effect on the electronic properties of the corresponding Ru(II) complexes. The oxidation strength of the ^{3}MLCT excited states can be tuned over a range of 900 mV. The lifetime of the most oxidizing excited state is 255 ns at room temperature, making this complex an excellent candidate for thermodynamically challenging photodriven oxidative chemistry.

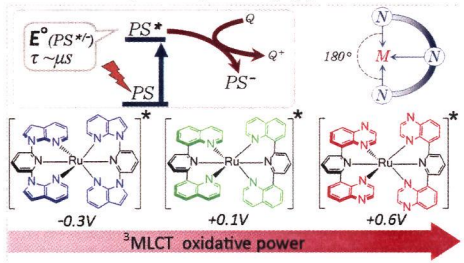

5138 dx.doi.org/10.1021/ic400015v

Remarkable Inertness of Copper(II) Chelates of Cyclen-Based Macrobicycles with Two *trans-N*-Acetate Arms

Catarina V. Esteves, Pedro Lamosa, Rita Delgado,* Judite Costa, Pauline Désogère, Yoann Rousselin, Christine Goze, and Franck Denat*

Two cross-bridged cyclen-based macrocycles with *trans-N*-acetic acid arms, H_2L1 and H_2L2, together with some of their complexes were synthesized and characterized. Both compounds behave as "proton sponges" and exhibit an excellent selectivity for copper(II). The [CuL1] and [CuL2] complexes are extremely inert to demetallate, especially [CuL2] ($t_{1/2}$ = 30.8 d in 12 M HCl and 363.2 K). The acetate arms play an important role during the formation of the complexes.

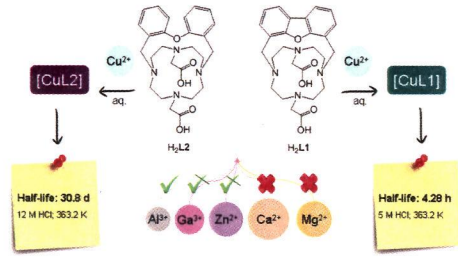

5154 dx.doi.org/10.1021/ic4000395

3c/4e *ô*-Type Long-Bonding: A Novel Transitional Motif toward the Metallic Delocalization Limit

C. R. Landis* and F. Weinhold

The surprising "long-bond" and "long-antibond" motifs, in which distant ligands appear to be bonded or even antibonded to one another, can represent the dominant resonance contributors in three center bonding interactions. The nature of the long-bonding interaction and its role in stabilizing triads of low electronegativity elements such as $BeLi_2$ and $ZnCu_2$ can be understood in the context of filled donor−acceptor interactions rather than real bonds between distant atoms.

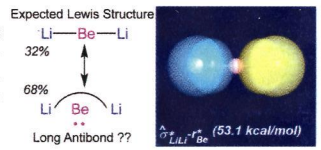

5167 dx.doi.org/10.1021/ic4000457

Spectroscopic and Phosphorescent Modulation in Triphosphine-Supported $PtAg_2$ Heterotrinuclear Alkynyl Complexes

Li-Yi Zhang, Liang-Jin Xu, Xu Zhang, Jin-Yun Wang, Jia Li, and Zhong-Ning Chen*

The phosphorescence in triphosphine-supported $PtAg_2$ heterotrinuclear alkynyl complexes was systematically modulated by structural modification and vapor of MeCN, pyridine, DMF, etc. with coordinating character.

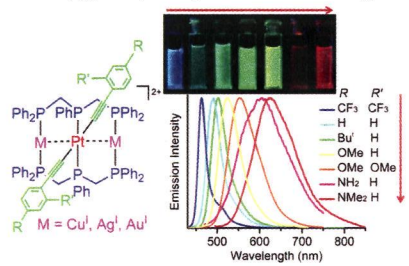

5176 dx.doi.org/10.1021/ic400458a

New Alkali-Metal Gallium Selenites, $AGa(SeO_3)_2$ (A = Li, Na, K, and Cs): Effect of Cation Size on the Framework Structures and Macroscopic Centricities

Dong Woo Lee and Kang Min Ok*

Four new alkali-metal gallium selenites materials, $AGa(SeO_3)_2$ (A = Li, Na, K, and Cs), have been synthesized by hydrothermal reactions. Cation size plays an important role in determining the framework structures and macroscopic centricities of the materials.

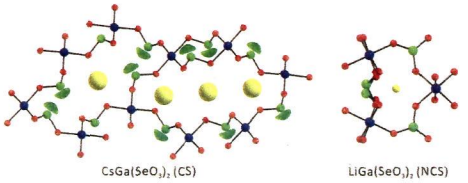

5185 dx.doi.org/10.1021/ic400077z

Phosphine and Diphosphine Complexes of Silicon(IV) Halides

William Levason,* David Pugh, and Gillian Reid

Six-coordinate adducts of SiX_4 (X = Cl or Br) with PMe_3 and various diphosphines are described and their properties compared with the germanium analogues. The first phosphine complex of a halosilane $[SiHCl_3\{Et_2P(CH_2)_2PEt_2\}]$ is also described, but SiX_4-arsine adducts could not be isolated.

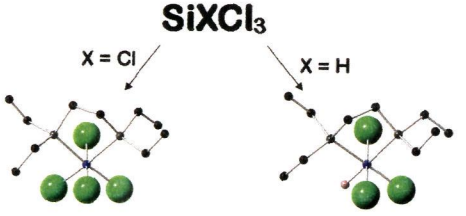

5194 dx.doi.org/10.1021/ic400098c

Subcomponent Self-Assembly of Rare-Earth Single-Molecule Magnets

Victoria E. Campbell,* Régis Guillot, Eric Riviere, Pierre-Thomas Brun, Wolfgang Wernsdorfer, and Talal Mallah

A family of lanthanide complexes has been synthesized by the subcomponent self-assembly methodology. Molecular architectures, which were stable in solution and under ambient conditions, were designed by the in situ formation of ligands around lanthanide ion templates. Magnetic studies indicated that **1** and **2** display single molecule magnet (SMM) behavior. Step-like features in the hysteresis loops indicate the presence of quantum tunneling of the magnetization (QTM).

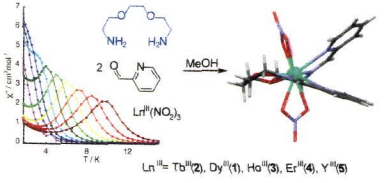

5201 dx.doi.org/10.1021/ic400102q

Tracking Reactive Intermediates by FTIR Monitoring of Reactions in Low-Temperature Sublimed Solids: Nitric Oxide Disproportionation Mediated by Ruthenium(II) Carbonyl Porphyrin Ru(TPP)(CO)

Arsen S. Azizyan, Tigran S. Kurtikyan,* Garik G. Martirosyan, and Peter C. Ford*

Interaction of NO (^{15}NO) with amorphous layers of Ru(II) carbonyl porphyrin was monitored by FTIR spectroscopy from 80 K to room temperature. An intermediate spectrally characterized at very low temperatures (110 K) with ν(CO) at 2001 cm^{-1} and ν(NO) at 1810 (1777 cm^{-1} for ^{15}NO isotopomer) was readily assigned to the mixed carbonyl−nitrosyl complex Ru(TPP)(CO)(NO), which is the logical precursor to CO labilization.

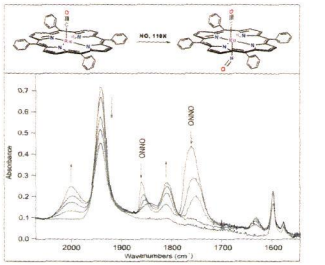

5206 dx.doi.org/10.1021/ic400111w

Interlayer Switching of Reduction in Layered Oxide, $Bi_4V_2O_{11-\delta}$ ($0 \leq \delta \leq 1$)

Yaoqing Zhang* and Yutaka Ueda

With increasing oxygen deficiency in $Bi_4V_2O_{11-\delta}$, the site that is reduced would be switched from the vanadate layer to the bismuthate layer leading to the formation of bismuth deficient phases.

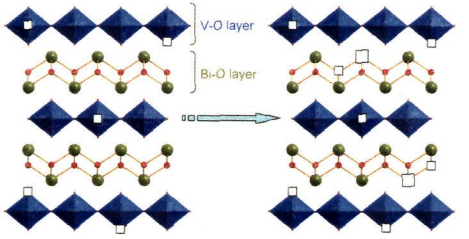

5214 dx.doi.org/10.1021/ic4001285

On the Synthesis and Reactivity of Highly Labile Pseudohalogen Phosphenium Ions

Christian Hering, Axel Schulz,* and Alexander Villinger

The synthesis and characterization of salts bearing highly labile pseudohalogen-substituted aminophosphenium cations of the type $[(Me_3Si)_2NPX][GaCl_4]$ (X = NCO, NCS, $O(SiMe_3)$) and their reactivity toward Lewis bases and dienes are described.

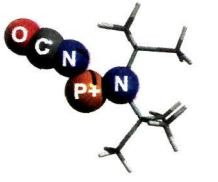

5226 (S) dx.doi.org/10.1021/ic4001413

Heme Bound Amylin: Spectroscopic Characterization, Reactivity, and Relevance to Type 2 Diabetes

*Soumya Mukherjee and Somdatta Ghosh Dey**

Heme binds to human amylin or islet amyloid polypeptide (hIAPP) via His18, in the presence of Arg11 which hydrogen bonds to the propionate side chains of the heme, with a trans-axial water derived ligand to form a high-spin active site. The reduced heme-hIAPP complexes generate reactive oxygen species and oxidative stress, significant to the pathology of type 2 diabetes mellitus.

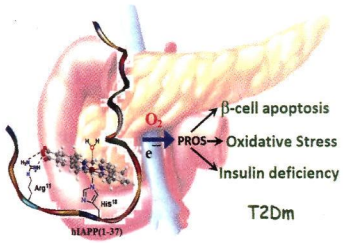

5236 (S) dx.doi.org/10.1021/ic400171z

Sequential Oxidations of Thiolates and the Cobalt Metallocenter in a Synthetic Metallopeptide: Implications for the Biosynthesis of Nitrile Hydratase

Arnab Dutta, Marco Flores, Souvik Roy, Jennifer C. Schmitt, G. Alexander Hamilton, Hilairy E. Hartnett, Jason M. Shearer, and Anne K. Jones*

Air oxidation of the cobalt-bound seven amino acid peptide ACDLPCG (Co-SODA) is characterized as a model for maturation of nitrile hydratase. Co-SODA is oxidized in two steps. In the first step, the metallocenter remains unchanged while one of the thiolates is oxidized to sulfinate. In the second step, the cobalt center is oxidized to Co^{3+}.

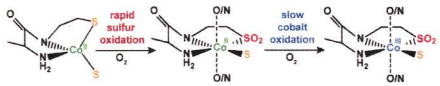

5246 (S) dx.doi.org/10.1021/ic400174r

Monopicolinate-dipicolyl Derivative of Triazacyclononane for Stable Complexation of Cu^{2+} and $^{64}Cu^{2+}$

Melissa Roger, Luís M. P. Lima, Mathieu Frindel, Carlos Platas-Iglesias,* Jean-François Gestin, Rita Delgado,* Véronique Patinec, and Raphaël Tripier*

The synthesis and characterization of H**no1pa2py**, a new tacn-based ligand, is reported. The complexation process with Cu^{2+} was proved to be very fast even in acidic medium. Potentiometric titrations allowed us to establish that H**no1pa2py** exhibits an overall low basicity as well as a high selectivity for Cu^{2+} over Zn^{2+} cations. The copper(II) complex was synthesized and characterized using UV−vis and EPR spectroscopies and density functional theory (DFT) calculations.

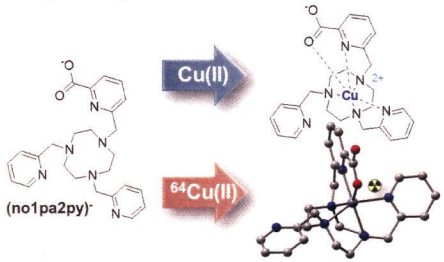

5260 (S) dx.doi.org/10.1021/ic400186x

$V^{IV}O$ Versus V^{IV} Complex Formation by Tridentate (O, N_{arom}, O) Ligands: Prediction of Geometry, EPR ^{51}V Hyperfine Coupling Constants, and UV−Vis Spectra

Luisa Pisano, Katalin Várnagy, Sarolta Timári, Kaspar Hegetschweiler, Giovanni Micera, and Eugenio Garribba*

Systems formed using the $V^{IV}O^{2+}$ ion with tridentate ligands containing a (O, N_{arom}, O) donor set were described. Examined ligands were 3,5-bis(2-hydroxyphenyl)-1*H*-1,2,4-triazole (H_2hyph^{Ph}), 4-[3,5-bis(2-hydroxyphenyl)-1,2,4-triazol-1-yl]-benzoic acid (H_3hyph^{C}), 4-[3,5-bis(2-hydroxyphenyl)-1,2,4-triazol-1-yl]-sulfonic acid (H_3hyph^{S}), and 2,6-bis(2′-hydroxyphenyl)-pyridine (H_2bhpp), with H_3hyph^{C} being an orally active iron chelator that is commercially available under the name Exjade (Novartis) for treatment of chronic iron overload arising from blood transfusions.

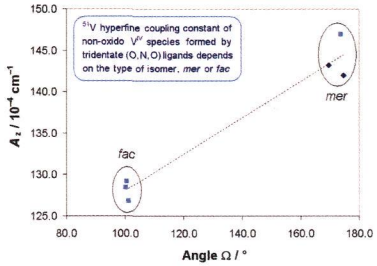

5273 (S) dx.doi.org/10.1021/ic400196a

Enhancing the Anion Affinity of Urea-Based Receptors with a $Ru(terpy)_2^{2+}$ Chromophore

Giorgio Baggi, Massimo Boiocchi, Carlo Ciarrocchi, and Luigi Fabbrizzi*

Covalent linking of a $Ru(terpy)_2^{2+}$ substituent enhances urea's affinity toward anions to a larger extent than classical electron-withdrawing groups like nitrophenyl and favors N−H deprotonation in the presence of excess fluoride.

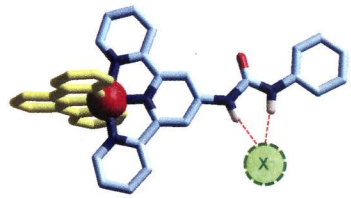

5284 (S) dx.doi.org/10.1021/ic400713p

Ferrocene-*o*-Benzosemiquinonato Tin(IV) Electron-Transfer Complexes

Ekaterina V. Ilyakina, Andrey I. Poddel'sky,* Georgy K. Fukin, Artem S. Bogomyakov, Vladimir K. Cherkasov, and Gleb A. Abakumov

The first examples of electron-transfer systems containing ferrocene and a nontransition metal complex based on redox-active ligands: ferrocene−*o*-benzosemiquinonato tin(IV) complexes $[(3,6\text{-Cat})SnBr_3]^-[Cp_2Fe]^+$ and $[(3,6\text{-Cat})(3,6\text{-SQ})SnCl_2]^-[Cp_2Fe]^+$ are reported. The interaction between ferrocene and *o*-benzosemiquinonato tin(IV) halides is reversible and depends on the solvent media. The structures of both electron-transfer complexes were confirmed by X-ray analysis. Complex $[(3,6\text{-Cat})(3,6\text{-SQ})SnCl_2]^-[Cp_2Fe]^+$ demonstrates the ferromagnetic coupling in the linear chain alternating $\cdots D^+{}^\bullet A^-{}^\bullet D^+{}^\bullet A^-{}^\bullet\cdots$ motif.

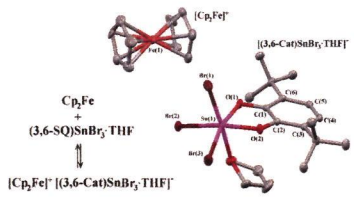

5290 S dx.doi.org/10.1021/ic400237h

Coordination Chemistry of 6-Thioguanine Derivatives with Cobalt: Toward Formation of Electrical Conductive One-Dimensional Coordination Polymers

Pilar Amo-Ochoa, Simone S. Alexandre, Samira Hribesh, Miguel A. Galindo, Oscar Castillo, Carlos J. Gómez-García, Andrew R. Pike, José M. Soler, Andrew Houlton,* and Félix Zamora*

Five cobalt complexes with 6-thioguanine (6-ThioGH) 6-thioguanosine (6-Thio-GuoH), or 2′-deoxy-6-thioguanosine (2′-d-6-ThioGuoH) ligands have been isolated and X-ray characterized. These ligands coordinate to cobalt *via* N7 and S6 forming a chelate ring. While 6-ThioGH forms monodimensional cobalt(II) coordination polymers, 2′-d-6-ThioGuoH and 6-ThioGuoH give rise to mononuclear cobalt complexes which form extensive H-bonds interactions to generate 3D supramolecular networks. The electrical and magnetic properties of the coordination polymers isolated have been studied.

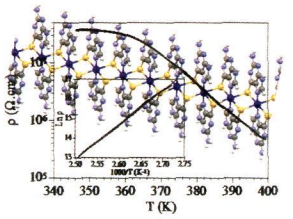

5300 S dx.doi.org/10.1021/ic400246y

(α-DT-TTF)$_2$[Au(mnt)$_2$]: A Weakly Disordered Molecular Spin-Ladder System

Rafaela A. L. Silva, Ana I. S. Neves, Elsa B. Lopes, Isabel C. Santos, Joana T. Coutinho, Laura C. J. Pereira, Concepció Rovira, Manuel Almeida,* and Dulce Belo*

(α-DT-TTF)$_2$[Au(mnt)$_2$] is a still rare example of an organic spin-ladder. In spite of the conformational disorder of the α-DT-TTF units, the magnetic behavior is preserved, due to the negligible electronic density of the HOMO in the thiophenic sulfur atoms, providing an interesting example of a weakly disordered spin-ladder.

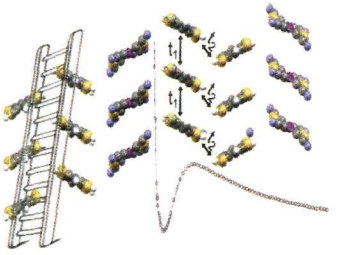

5307 S dx.doi.org/10.1021/ic400254v

Correlations between Chemical Bonding and Magnetic Exchange Interactions: Synthesis, Crystal Structures, and Magnetic Properties of the New Family RE_2AlGe_2 (RE = Tb−Tm, Lu)

Jiliang Zhang and Svilen Bobev*

The new rare-earth metal aluminum germanides with the formula RE_2AlGe_2 (RE = Tb−Tm, Lu) have been investigated. Their structure belongs to the orthorhombic W_2CoB_2-type structure and has a close relationship with the hexagonal AlB_2-type structure. The correlations between the chemical bonding and the magnetic exchange interactions have been rationalized based on the mean-field theory and two-lattice model for antiferromagnets.

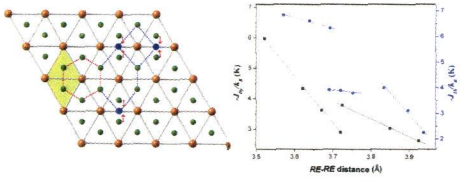

5316 S dx.doi.org/10.1021/ic4002576

Replica of a Fishy Enzyme: Structure−Function Analogue of Trimethylamine-N-Oxide Reductase

Golam Moula, Moumita Bose, and Sabyasachi Sarkar*

Mo(IV) stabilized by asymmetric bis dithiolene coordination similar to P and Q pterin coordinated to the native enzymes showed enzymatic saturation kinetics reaction of TMANOR.

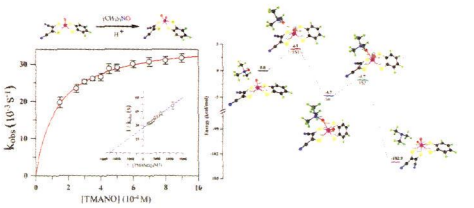

5328 S dx.doi.org/10.1021/ic4002626

Transferrin Serves As a Mediator to Deliver Organometallic Ruthenium(II) Anticancer Complexes into Cells

Wei Guo, Wei Zheng, Qun Luo, Xianchan Li, Yao Zhao, Shaoxiang Xiong, and Fuyi Wang*

Binding to human serum transferrin (hTf) has little effect on cellular uptake and bioavailability of ruthenium arene anticancer complexes and well preserves the cytotoxicity of the drug candidates. In contrast, the binding of cisplatin to hTf is irreversible and dramatically reduces its cytotoxicity. It is therefore feasible to use iron-loaded hTf as a mediator for targeting delivery of the organometallic ruthenium anticancer complexes and for circumventing the potential drug resistance resulting from protein bindings in endosomal and cytosolic compartments.

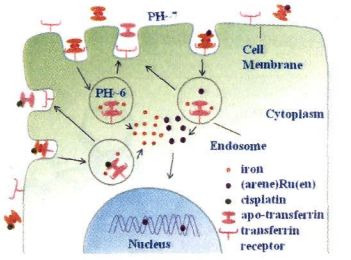

5339 S dx.doi.org/10.1021/ic4002658

Xantphos-Type Complexes of Group 9: Rhodium versus Iridium

Miguel A. Esteruelas,* Montserrat Oliván, and Andrea Vélez

While the chemistry of rhodium with 9,9-dimethyl-4,5-bis(diisopropylphosphino)xanthene is governed by d^8 square-planar complexes, that of iridium is centered on d^6 octahedral derivatives

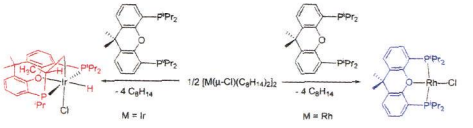

5350 (S) dx.doi.org/10.1021/ic400287g

Synthesis and Coordination Behavior of a Bipyridine Platinum(II) Complex with Thioglucose

Takaaki Tsuji, Naoto Kuwamura, Nobuto Yoshinari, and Takumi Konno*

A mononuclear platinum(II) complex with two monodentate-*S* H_4tg^- ligands, $[Pt(H_4tg\text{-}\kappa S)_2(bpy)]$ (**1**), was synthesized by the reaction of $[PtCl_2(bpy)]$ (bpy = 2,2′-bipyridyl) with NaH_4tg (NaH_4tg =1-thio-β-d-glucose sodium salt) in water. Complex **1** reacted with additional $[PtCl_2(bpy)]$ in water to give $[Pt_2(\mu_2\text{-}H_4tg\text{-}\kappa^1S{:}\kappa^1S)_2(bpy)_2]^{2+}$ ($[\mathbf{2}]^{2+}$). Treatments of **1** with Cu^{2+} and Ni^{2+} in water in the presence of bpy produced $[PtCu(\mu_2\text{-}H_4tg\text{-}\kappa^1S{:}\kappa^2O,S)_2(bpy)_2]^{2+}$ ($[\mathbf{3}]^{2+}$) and $[PtNi(\mu_2\text{-}H_4tg\text{-}\kappa^1S{:}\kappa^2O,S)_2(bpy)_2]^{2+}$ ($[\mathbf{4}]^{2+}$), and similar treatment with Cd^{2+} in the presence of bpy resulted in $[Cd\{Pt(\mu_2\text{-}H_4tg\text{-}\kappa^1S{:}\kappa^2O,S)(\mu_2\text{-}H_4tg\text{-}\kappa^1S{:}\kappa^1S)(bpy)\}_2]^{2+}$ ($[\mathbf{5}]^{2+}$).

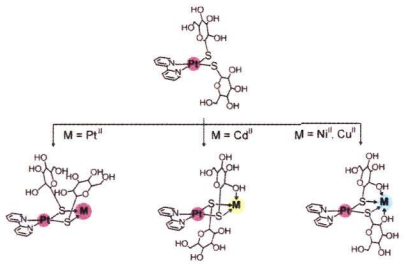

5359 (S) dx.doi.org/10.1021/ic4002779

New Salt-Inclusion Borate, $Li_3Ca_9(BO_3)_7{\cdot}2[LiF]$: A Promising UV NLO Material with the Coplanar and High Density BO_3 Triangles

Hongwei Yu, Hongping Wu, Shilie Pan,* Ying Wang, Zhihua Yang, and Xin Su

A new salt-inclusion borate, $Li_3Ca_9(BO_3)_7{\cdot}2[LiF]$, was synthesized with the spontaneous nucleation technique. Owing to possessing coplanar and high density BO_3 triangles in the structure, it exhibits a moderate SHG response, a wide transparent region, and large birefringence, which will be favorable for its practical application as a UV NLO material.

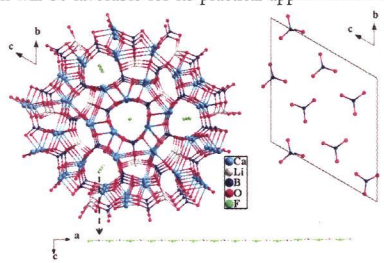

5366 (S) dx.doi.org/10.1021/ic4003548

Synthesis, Steady-State, and Femtosecond Transient Absorption Studies of Resorcinol Bound Ruthenium(II)- and Osmium(II)-polypyridyl Complexes on Nano-TiO_2 Surface in Water

Tanmay Banerjee, Sreejith Kaniyankandy, Amitava Das,* and Hirendra Nath Ghosh*

The synthesis of two new ruthenium(II)- and osmium(II)-polypyridyl complexes, with resorcinol as the enediol anchoring moiety, is described. Femtosecond transient absorption studies have been carried out on the dye–TiO_2 systems in water to reveal <120 fs and 1.5 ps electron injection times along with 30% slower BET time for the ruthenium complex. However, the corresponding osmium complex shows strikingly different behavior for which only a <120 fs ultrafast injection is observed. Most remarkably, the back electron transfer is faster as compared to the corresponding catechol analogue of the dye.

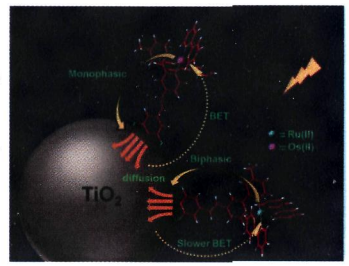

5378 (S) dx.doi.org/10.1021/ic4003324

$Zn_2(VO_4)(IO_3)$: A Novel Polar Zinc(II) Vanadium(V) Iodate with a Large SHG Response

Bing-Ping Yang, Chun-Li Hu, Xiang Xu, Chao Huang, and Jiang-Gao Mao*

The first zinc(II) vanadium(V) iodate, namely, $Zn_2(VO_4)(IO_3)$, has been prepared and structurally characterized. It displays a novel 3D network structure composed of ZnO_5, ZnO_6, VO_4, and IO_3 polyhedra, in which 1D chains of edge-sharing ZnO_5 polyhedra and 1D chains of corner-sharing ZnO_6 octahedra along the *c*-axis are interconnected via corner-sharing into 2D zinc oxide layers with VO_4 tetrahedra and IO_3 groups as interlayer linkers. Results of powder SHG measurements indicate that $Zn_2(VO_4)(IO_3)$ exhibits a large response of ~6 × KDP and is Type I phase-matchable.

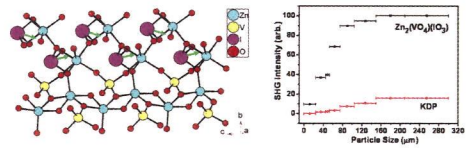

5385 (S) dx.doi.org/10.1021/ic400337m

Synthesis, Structure, and Solution Reduction Reactions of Volatile and Thermally Stable Mid to Late First Row Transition Metal Complexes Containing Hydrazonate Ligands

Lakmal C. Kalutarage, Philip D. Martin, Mary Jane Heeg, and Charles H. Winter*

The hydrazonate complexes $M(tBuNNCHCtBuO)_2$ (M = Ni, Co, Fe, Mn, Cr), $M(tBuNNCHCiPrO)_2$ (M = Ni, Co, Fe), and $M(tBuNNCMeCMeO)_2$ (M = Ni, Co, Fe) have been prepared and fully characterized. These complexes have very promising properties for use as precursors in the growth of the metal films in atomic layer deposition processes.

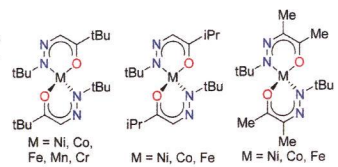

5395 S dx.doi.org/10.1021/ic400347r

Synthesis, Photo-, and Electrochemistry of Ruthenium Bis(bipyridine) Complexes Comprising a *N*-heterocyclic Carbene Ligand

Vivienne Leigh, Wadih Ghattas, Ralte Lalrempuia, Helge Müller-Bunz, Mary T. Pryce, and Martin Albrecht*

New analogues of $[Ru(bpy)_3]^{2+}$ with one pyridine ligand site substituted by different types of N-heterocyclic carbenes demonstrate spectroscopic, photophysical, and electrochemical properties that are attractive for utilization as photosensitizers. The smallest HOMO-LUMO gap was determined for the complex featuring a mesoionic triazolylidene as N-heterocyclic carbene ligand

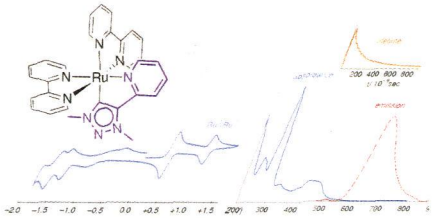

5403 S dx.doi.org/10.1021/ic400352r

Reversible Carbon–Carbon Bond Formation Induced by Oxidation and Reduction at a Redox-Active Cobalt Complex

Crisita Carmen Hojilla Atienza, Carsten Milsmann, Scott P. Semproni, Zoë R. Turner, and Paul J. Chirik*

The electronic structure of the diamagnetic pyridine imine enamide cobalt dinitrogen complex, $(^{iPr}PIEA)CoN_2$ ($^{iPr}PIEA$ = 2-(2,6-$^{i}Pr_2$–C_6H_3N=CMe)-6-(2,6-$^{i}Pr_2$–C_6H_3NC=CH_2)C_5H_3N), was determined and is best described as a low-spin cobalt(II) complex antiferromagnetically coupled to an imine radical anion.

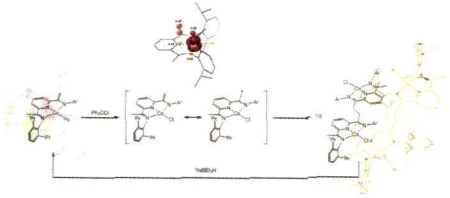

5418 S dx.doi.org/10.1021/ic400361s

Lewis-Acid-Promoted Stoichiometric and Catalytic Oxidations by Manganese Complexes Having Cross-Bridged Cyclam Ligand: A Comprehensive Study

Lei Dong, Yujuan Wang, Yanzong Lv, Zhuqi Chen, Fuming Mei, Hui Xiong, and Guochuan Yin*

This work presents how redox-inactive metal ions affect the oxidative reactivities of the $Mn(Me_2EBC)$ complexes. Adding these metal ions would greatly accelerate the electron transfer rate of the manganese complexes, and acceleration is highly Lewis-acid strength dependent on added metal ions, while its hydrogen abstraction and oxygen transfer efficiencies are just slightly improved. Improvements are related with formation of the Mn(IV)–O–Lewis-acid unit, which increases its potential and oxidizing ability.

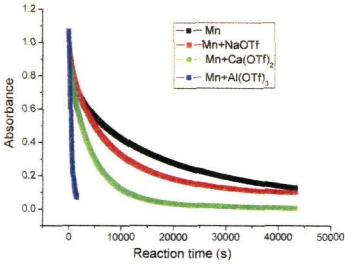

5428 S dx.doi.org/10.1021/ic4003687

Synthesis and Reactivity of New Rhenium(I) Complexes Containing Iminophosphorane-Phosphine Ligands: Application to the Catalytic Isomerization of Propargylic Alcohols in Ionic Liquids

Joaquín García-Álvarez,* Josefina Díez, José Gimeno, Christine M. Seifried, and Cristian Vidal

New iminophosphorane–phosphine Re(I) complexes have been synthesized and used for the catalytic isomerization of terminal propargylic alcohols into α,β-unsaturated enals or methylketones under neutral conditions, using the ionic liquid $[BMIM][PF_6]$ as a nonconventional solvent. This catalytic system could be recycled up to 10 consecutive times. Isolation and X-ray characterization of the key intermediate rhenium(I) oxacyclocarbene complex (A) seems to indicate that the catalytic reaction proceeds through tautomerization of the terminal alkynols to yield vinylidene-type species.

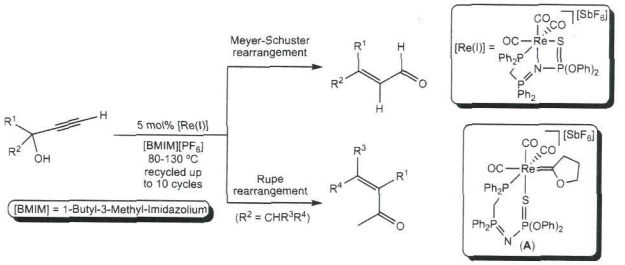

5438 Ⓢ dx.doi.org/10.1021/ic4003737

Acrylic Acid Derivatives of Group 8 Metal Carbonyls: A Structural and Kinetic Study

Bo Li, Samuel J. Kyran, Andrew D. Yeung, Ashfaq A. Bengali,* and Donald J. Darensbourg*

The synthesis of group 8 metal carbonyl acrylic acid and its conjugate base derivatives are reported which are fully characterized by spectroscopic and X-ray crystallographic analyses. Ligand replacement kinetics of the olefinic ligands via PPh_3 were carried out which are consistent with a dissociative reaction pathway. In accordance with this interpretation, enthalpies of activation were shown to correlate with bond dissociation energies (BDEs) determined by DFT computations. Chemistry relevant to the coupling of CO_2 and ethylene for the production of acrylic acid is discussed.

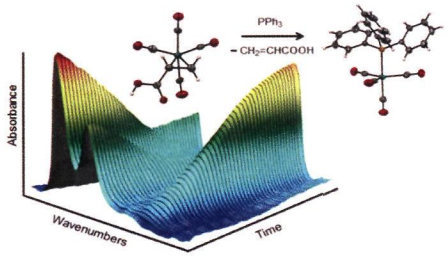

5448 Ⓢ dx.doi.org/10.1021/ic4003753

Synthesis of New Late Transition Metal P,P-, P,N-, and P,O- Complexes Using Phosphonium Dimers as Convenient Ligand Precursors

Kanghee Park, Paraskevi O. Lagaditis, Alan J. Lough, and Robert H. Morris*

A phosphine aldehyde, generated in situ from a phosphonium dimer under basic conditions, is used as a ligand precursor for the synthesis of chelating phosphino-enolate, -imine, and -oxime ligands, as well as the monodentate phosphine ligand with a pendant aldehyde. P−O and P−N complexes synthesized using $[M(cod)Cl]_2$ metal precursors (M = Rh(I), Ir(I)) showed activity for olefin hydrogenation.

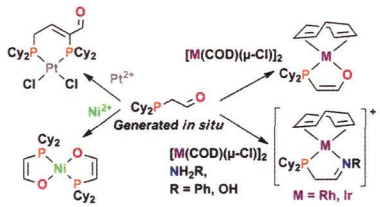

5457 Ⓢ dx.doi.org/10.1021/ic400348j

Synthesis and Electrochemical Reactivity of Molybdenum Dicarbonyl Supported by a Redox-Active α-Diimine Ligand

Isaac R. Corn, Pablo D. Astudillo-Sánchez, Michael J. Zdilla, Phillip E. Fanwick, Michael J. Shaw, Jeffrey T. Miller, Dennis H. Evans,* and Mahdi M. Abu-Omar*

Structural and spectral features of molybdenum dicarbonyl complexes supported by a redox-active diimine ligand are described. Despite variation in the ligand bond lengths in the complexes, X-ray absorption spectroscopy establishes molybdenum(0) as the oxidation state. Electrochemical studies of the title compound reveal an electrochemical−chemical process in which the dicarbonyl ligands undergo cis-to-trans isomerization.

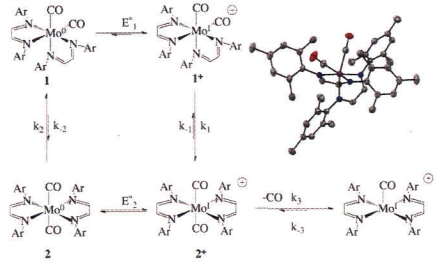

5464 dx.doi.org/10.1021/ic400376g

Pressure-Induced Transformations in $PrVO_4$ and $SmVO_4$ and Isolation of High-Pressure Metastable Phases

Daniel Errandonea,* S. Nagabhusan Achary, Julio Pellicer-Porres, and Avesh K. Tyagi

Zircon-type $PrVO_4$ and $SmVO_4$ have been studied by high-pressure Raman spectroscopy up to 17 GPa. The occurrence of phase transitions has been detected when compression exceeds 6 GPa. The transformations are not reversible. Raman spectra of the high-pressure phases show similarities with those expected for a monazite-type phase in $PrVO_4$ and a scheelite-type phase in $SmVO_4$. X-ray diffraction measurements of the metastable products recovered after decompression confirms the monazite ($PrVO_4$) and scheelite ($SmVO_4$) structures of the high-pressure phases.

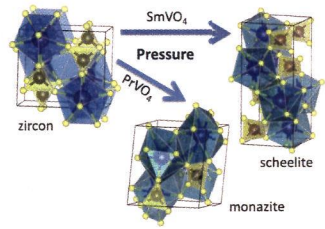

5470 Ⓢ dx.doi.org/10.1021/ic400377k

Next Generation PhotoCORMs: Polynuclear Tricarbonylmanganese(I)-Functionalized Polypyridyl Metallodendrimers

Preshendren Govender, Sandesh Pai, Ulrich Schatzschneider,* and Gregory S. Smith*

Two generations of CO-releasing poly(propyleneimine-bipyridylimine) metallodendrimers incorporating $Mn(CO)_3$ units on the periphery have been synthesized and characterized. The CO-release properties of these metallodendrimers were investigated in pure buffer, using the myoglobin assay. A mononuclear model complex was also synthesized and studied with the aid of DFT/TDDFT calculations

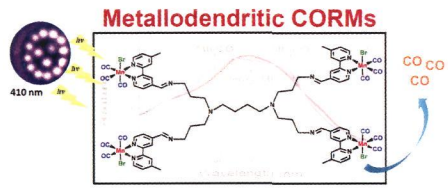

5479 dx.doi.org/10.1021/ic400381g

Lone Pair Effect, Structural Distortions, and Potential for Superconductivity in Tl Perovskites

Leslie M. Schoop,* Lukas Müchler, Claudia Felser, and R. J. Cava

Drawing an analogy between $BaBiO_3$ and Tl halide perovskites, we show that superconductivity is possible in the latter. We investigate the effect of symmetry on electronic properties and chemical stability.

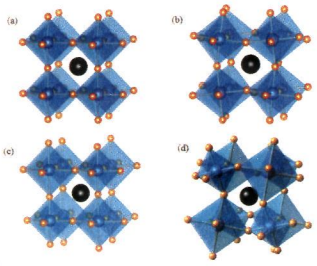

5484 dx.doi.org/10.1021/ic400383t

Boron-Dipyrromethene-Functionalized Hemilabile Ligands as "Turn-On" Fluorescent Probes for Coordination Changes in Weak-Link Approach Complexes

Alejo M. Lifschitz, Chad M. Shade, Alexander M. Spokoyny, Jose Mendez-Arroyo, Charlotte L. Stern, Amy A. Sarjeant, and Chad A. Mirkin*

Hemilabile ligands consisting of phosphino-thioether and phosphino-amine moieties linked to Bodipy fluorophores via phenylene bridges were used to signal coordination changes at Pt(II) metal centers. The ligands allow for "turn-on" fluorescence signaling of both ligand chelation and ligand displacement reactions in a quantitative fashion. The complexes are models for sensing and signal amplification constructs assembled by the weak-link approach.

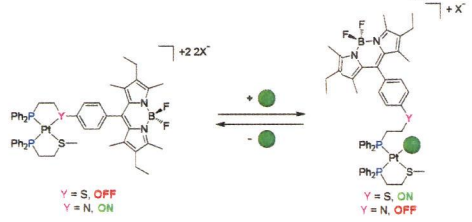

5493 dx.doi.org/10.1021/ic4004005

Oxidatively Induced P–O Bond Formation through Reductive Coupling between Phosphido and Acetylacetonate, 8-Hydroxyquinolinate, and Picolinate Groups

Andersson Arias, Juan Forniés, Consuelo Fortuño,* Antonio Martín, Piero Mastrorilli,* Stefano Todisco, Mario Latronico, and Vito Gallo

The oxidation of palladium and platinum(II) phosphanido derivatives with *O*-donor ligands allows identification of intermediates in formal oxidation states Pt(III)(square-planar)-Pt(III)(square-planar) or Pt(II)(square-planar)–Pt(IV)-(octahedral). The Pt(II),Pt(IV) intermediates evolve through reductive coupling with formation of P–O bonds resulting in new phosphane ligands Ph_2P-hq, Ph_2P-pic, and Ph_2P-acac.

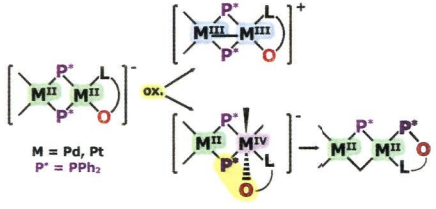

5507 dx.doi.org/10.1021/ic400412f

Synthesis and Characterization of an Azido-Bridged Dinuclear Ruthenium(II) Polypyridylamine Complex Forming a Mixed-Valence State

Misaki Makino, Tomoya Ishizuka, Shingo Ohzu, Jiang Hua, Hiroaki Kotani, and Takahiko Kojima*

In the crystal structure of a dinuclear ruthenium(II) μ-azido complex having a pentadentate poly(pyridylmethyl)amine as an ancillary ligand, intramolecular $\pi-\pi$ stacking was found between the pyridine rings of the two ancillary ligands, contributing to stabilize the dinuclear μ-azido structure. The μ-azido complex was revealed to exhibit a stepwise oxidation behavior in CH_3CN to afford a $Ru^{II}-\mu$-azido$-Ru^{III}$ mixed-valence (MV) state upon one-electron oxidation. The MV state was categorized in the Robin–Day class II.

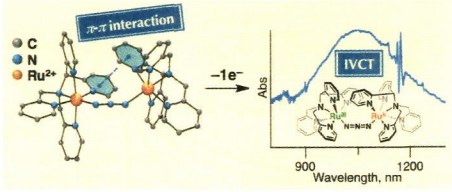

5515 dx.doi.org/10.1021/ic400420h

Inorganic and Organozinc Fluorocarboxylates: Synthesis, Structure and Materials Chemistry

A. L. Johnson, A. J. Kingsley, G. Kociok-Köhn, K. C. Molloy,* and A. L. Sudlow

The organozinc fluorocarboxylates $RZnO_2CR_f$, $RZnO_2CR_f$·TMEDA, and $Zn(O_2CR_f)_2$·TMEDA (R = Me, Et; $R_f \simeq C_2F_5$, C_3F_7) have been synthesized and representative examples structurally characterized. While $EtZnO_2CC_2F_5$ decomposes in the bulk to ZnF_2, under LPCVD conditions $MeZnO_2CC_3F_7$ and $MeZnO_2CC_3F_7$·TMEDA give highly oriented, but fluorine-free, ZnO.

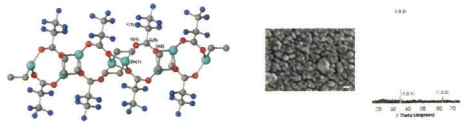

5527 dx.doi.org/10.1021/ic400448x

An Asymmetrically Derivatized 1,2,3-Triphospholide: Synthesis and Reactivity of the 4-(2′-Pyridyl)-1,2,3-triphospholide Anion

Robert S. P. Turbervill and Jose M. Goicoechea*

The synthesis of the 4-(2′-pyridyl)-1,2,3-triphospholide anion ($[P_3C_2H(2\text{-}C_5H_4N)]^-$; **1**) is reported. Preliminary coordination studies have shown that reactions of **1** with $Mo(CO)_6$ or $Mo(py)_3(CO)_3$ yield the diamagnetic piano-stool complex $[\{\eta^5\text{-}P_3C_2H(2\text{-}C_5H_4N)\}Mo(CO)_3]^-$ (**2**). By contrast, reaction of **1** with $Mo(COD)(CO)_4$ yields $[\{\kappa^2P,N\text{-}P_3C_2H(2\text{-}C_5H_4N)\}\text{-}Mo(CO)_4]^-$ (**3**) which readily loses a carbonyl on heating to give **2**. Reaction of **2** with $Mo(COD)(CO)_4$ affords the bimetallic system $[\{\mu:\eta^5,\kappa^2P,N\text{-}P_3C_2H(2\text{-}C_5H_4N)\}\{Mo(CO)_3\}\{Mo(CO)_4\}]^-$ (**4**).

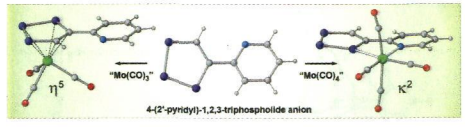

5535 S dx.doi.org/10.1021/ic400470g

Paramagnetic One-Dimensional Chains Comprised of Trinuclear Pt–Cu–Pt and Paddlewheel Dirhodium Complexes with Metal–Metal Bonds

Kazuhiro Uemura* and Masahiro Ebihara

Unique one-dimensional (1D) chain complexes comprised of three types of metal species, rhodium, platinum, and copper, are shown. These compounds are constructed of a dinuclear rhodium complex and a trinuclear Pt–Cu–Pt complex, forming attractive paramagnetic quasi-1D infinite chains. Interestingly, an unusual seven splittings in the EPR spectrum indicates that the unpaired spin on Cu is perturbed by the Pt atoms.

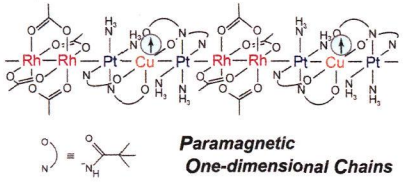

5551 S dx.doi.org/10.1021/ic400504h

Energetic Bis(3,5-dinitro-1*H*-1,2,4-triazolyl)dihydro- and dichloroborates and Bis(5-nitro-2*H*-tetrazolyl)-, Bis(5-(trinitromethyl)-2*H*-tetrazolyl)-, and Bis(5-(fluorodinitromethyl)-2*H*-tetrazolyl)dihydroborate

Ralf Haiges, C. Bigler Jones, and Karl O. Christe**

Bis(3,5-dinitro-1*H*-1,2,4-triazolyl)dihydro- and dichloroborates and bis(5-nitro-2*H*-tetrazolyl)-, bis(5-trinitromethyl-2*H*-tetrazolyl)-, and bis(5-fluorodinitromethyl-2*H*-tetrazolyl)dihydroborates have been synthesized from hydroborates or chloroborates and the corresponding nitroazoles or nitroazolates, respectively. Poly(nitroazolyl)borates are promising candidates for a new class of environmentally benign energetic materials and high-oxygen carriers.

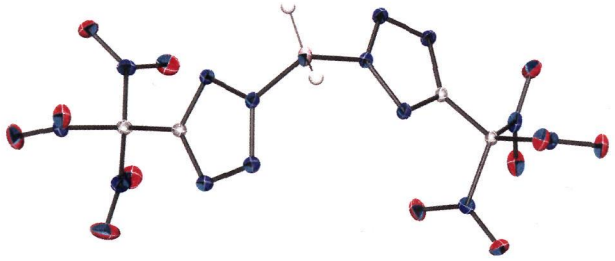

5559 S dx.doi.org/10.1021/ic400522z

Synthesis and Crystal Structures of Ca_4SiN_4 and New Polymorph of $Ca_5Si_2N_6$

Hisanori Yamane* and Haruhiko Morito

Single crystals of Ca_4SiN_4 were found in the product prepared by heating Ba, Ca, Si, NaN_3, and Na at 900 °C. Ca_4SiN_4 [space group $P2_1/c$ (No. 14), $Z = 4$, $a = 9.1905(4)$ Å, $b = 5.9775(3)$Å, $c = 11.0138(7)$ Å, $\beta = 116.4054(17)°$] is isotypic with Ca_4GeN_4 and K_4SiO_4. Isolated $[SiN_4]^{8-}$ tetrahedra were identified in the structure by single-crystal X-ray diffraction.

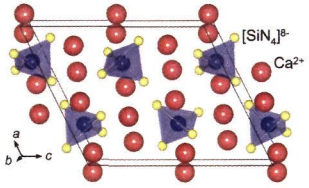

5564 dx.doi.org/10.1021/ic400525r

Lanthanides as NMR Probes of Fast Molecular Dynamics at High Magnetic Fields and Temperature Sensors: Conformational Interconversion of Erbium Ethylenediaminetetraacetate Complexes

Sergey P. Babailov,* Pavel A. Stabnikov, Eugeny N. Zapolotsky, and Vasily V. Kokovkin

The erbium ethylenediaminetetraacetate complex has been investigated using dynamic NMR methods. Intramolecular dynamics in complexes was assigned to the interconversion of Δ-λ_E-$\delta\delta\delta\delta$ and Δ-δ_E-$\delta\delta\delta\delta$ conformers with $\Delta G^{\ddagger}(298\ K) = 50 \pm 4$ kJ/mol. The coordination compound investigated in the paper represents a new type of thermometric NMR sensor.

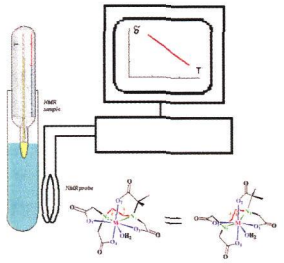

5570 S dx.doi.org/10.1021/ic400526j

A Polyaromatic Terdentate Binding Unit with Fused 5,6-Membered Chelates for Complexing s-, p-, d-, and f-Block Cations

Thi Nhu Y Hoang,* Marie Humbert-Droz, Thibault Dutronc, Laure Guénée, Céline Besnard, and Claude Piguet*

The two fused 5,6-membered chelate rings in the terdentate ligand **L7** *display considerable* binding affinity for protons, while the stability constants estimated for s-, d-, and f-block cations are moderate and surprisingly are not dependent on the electrostatic factors Z^2/R.

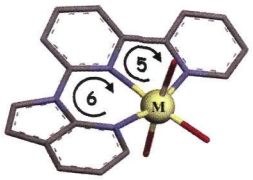

5581 S dx.doi.org/10.1021/ic4005455

Synthesis and Mössbauer Spectroscopy of Formal Tin(II) Dichloride and Dihydride Species Supported by Lewis Acids and Bases

S. M. Ibrahim Al-Rafia, Olena Shynkaruk, Sean M. McDonald, Sean K. Liew, Michael J. Ferguson, Robert McDonald, Rolfe H. Herber,* and Eric Rivard*

A series of tin(II) dichloride and dihydride adducts were analyzed by Mössbauer Effect spectroscopy to provide insight into the nature of the bonding environments in these species.

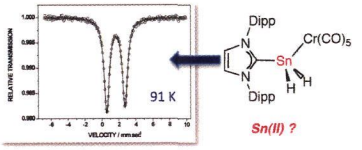

Ⓢ Supporting Information available via online article